Effects of the Indonesian Throughflow on Circulation of the Pacific Ocean

Tong Lee
Lee-Lueng Fu, Ichiro Fukumori, Ralf Giering, Dimitris Menemenlis, Zhangfan Xing

Jet Propulsion Laboratory, California Institute of Technology

Effects of the Indonesian Throughflow on the circulation and thermal structure of the Pacific Ocean are investigated using a global ocean general circulation model (OGCM) and various observations. The model is the parallel version of the MIT primitive equation OGCM. The meridional resolution is 0.3 degrees within 10 degrees of the equator, gradually increasing to 1 degree in the subtropics. The zonal resolution is 1 degree. There are 46 levels in the vertical, with 10 m resolution in the upper 150 m. The model, after spinup, was driven by real time NCEP reanalyzed surface fluxes from 1989 to 1997. Two experiments are conducted; one with open Indonesian passages and the other without. Comparisons were made between the two model solutions and with observational data from the TOGA-TAO arrays, WOCE hydrograhy, current meter moorings, etc.

With closed Indonesian passages, warm water from the Indonesian Seas (which would otherwise flow into the Indian Ocean with open passages) cause a systematic warming of the tropical Pacific thermocline resulting in large model deviations from observations, as shown in Figures 1 and 2. Wihtout the Throughflow, the Equatorial Undercurrent becomes weaker (Figures 3 and 4). Closing the passages has little effect on the exchange rate near 10N. However, the actual exchange between the tropical and northern subtropical Pacific is significantly smaller with open than with closed passages because a significant amount of thermocline water from the northern subtropical Pacific flows into the Indian Ocean through the Indonesian passageway. Exchange near 10S is affected more significantly by the closed passages than that near 10N, as seen from the changes in low-latitude boundary currents in Figure 4. Closing off the Indonesian Throughflow shifts the center of maximum variability in thermocline depth (as indicated by the depth of the 20 degree C isotherm), sea level, and sea surface temperature (Figures 5 and 6). The aforementioned changes have significant implications to implications to decadal variability.

Figure Captions:

Figure 1. Temperatures at 100 m depth with and without Indonesian Throughflow and their difference. The Pacific Ocean is warmed as a result of cloging the Indonesian Throughflow, especially in the eastern Pacific.

Figure 2. Zonal section of temperature at the equtor without and without Indonesian Throughflow and their difference. The waters above the thermocline is warmer without Indonesian Throughflow.

Figure 3. Meridional section of zonal velocity and temperature at 130E with and without Indonesian Throughflow and their differences, showing warmer waters and weaker Equatorial Undercurrent without the Indonesian Throughflow.

Figure 4. Zonal velocity map near the thermocline with and without Indonesian Throughflow and their difference, showing the effect of closing off the Indonesian Throughflow on low-latitude boundary currents which affects exchange of tropical and extra-tropical waters.

Figure 5. Difference in mean and r.m.s. variability of D20 (20 degree isotherm) with and without the Indonesian Throughflow.

Figure 6. Difference in mean and r.m.s. variability of sea surface temperature with and without the Indonesian Throughflow.

Acknowledgement:

The research described in this poster presentation was carried out by the Jet Propulsion Laboratory, California Institute of Technology, under a contract with the National Aeronautics and Space Administration.

Fig. 1

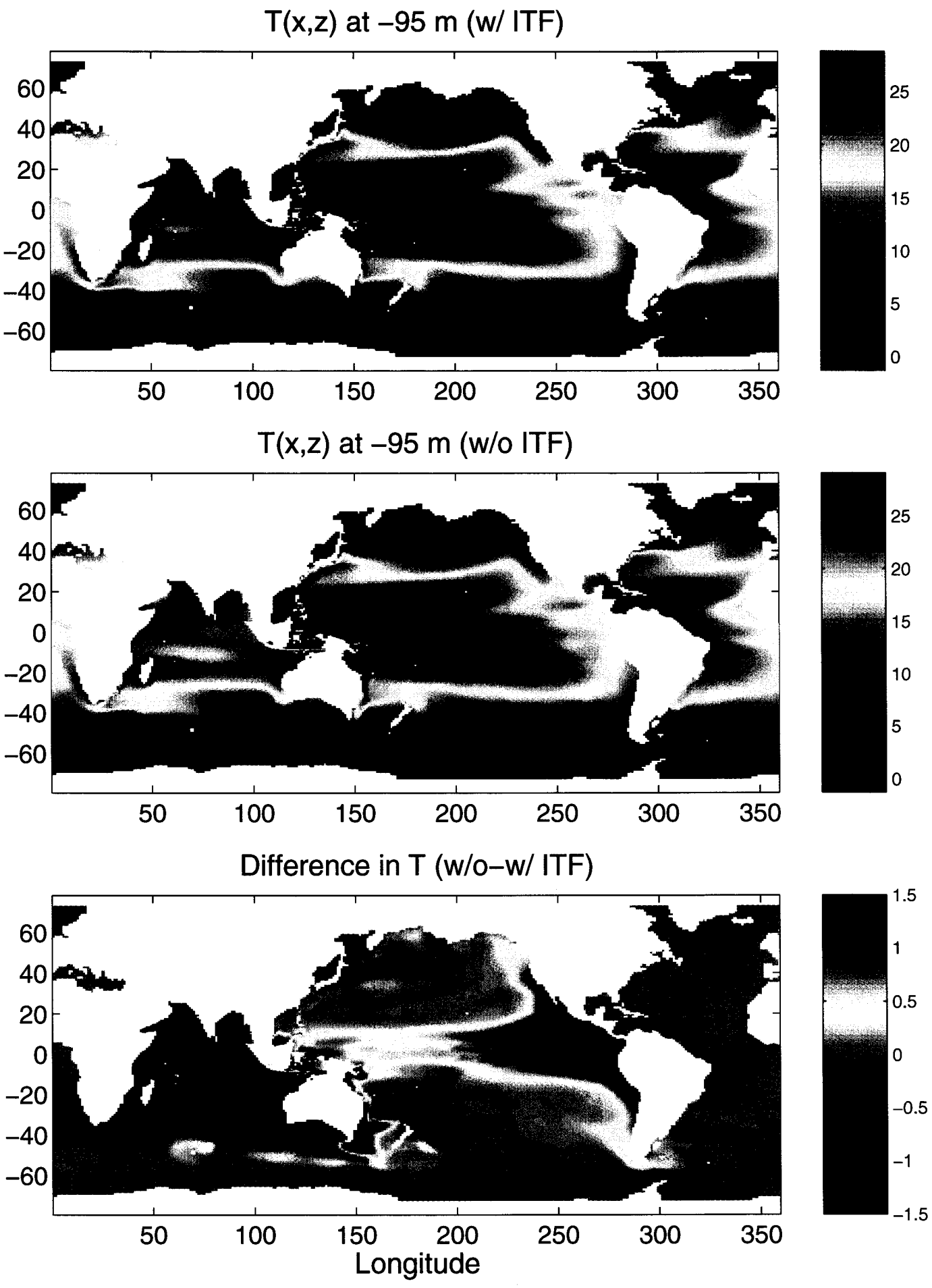
T(x,z) at −95 m (w/ ITF)
T(x,z) at −95 m (w/o ITF)
Difference in T (w/o−w/ ITF)
Latitude
Longitude
60
40
20
0
−20
−40
−60
50
100
150
200
250
300
350
25
20
15
10
5
0
1.5
1
0.5
0
−0.5
−1
−1.5

Fig. 2

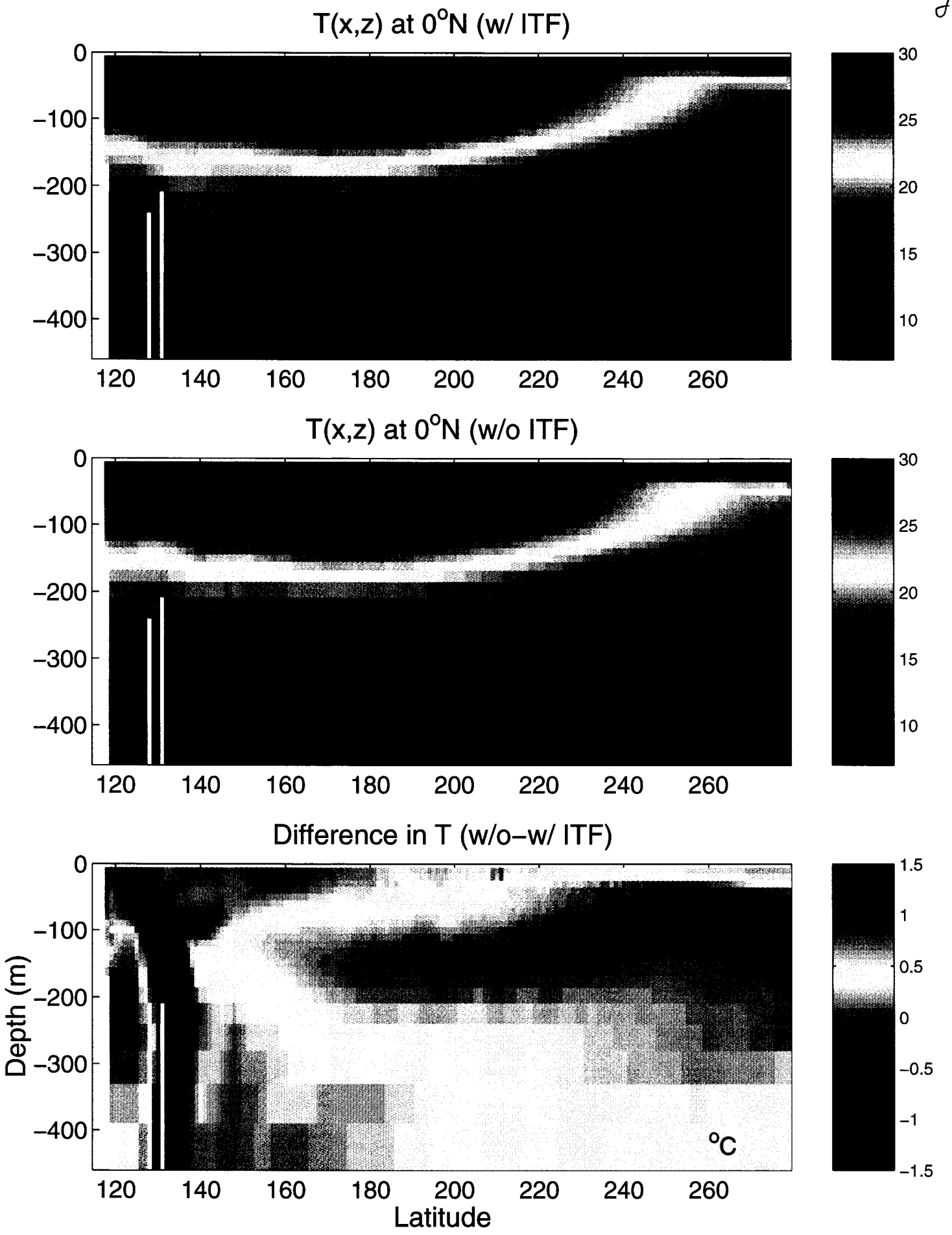
T(x,z) at 0°N (w/ ITF)
T(x,z) at 0°N (w/o ITF)
Difference in T (w/o–w/ ITF)
Depth (m)
Latitude
°C
0
−100
−200
−300
−400
120
140
160
180
200
220
240
260
30
25
20
15
10
1.5
1
0.5
0
−0.5
−1
−1.5

Fig. 3

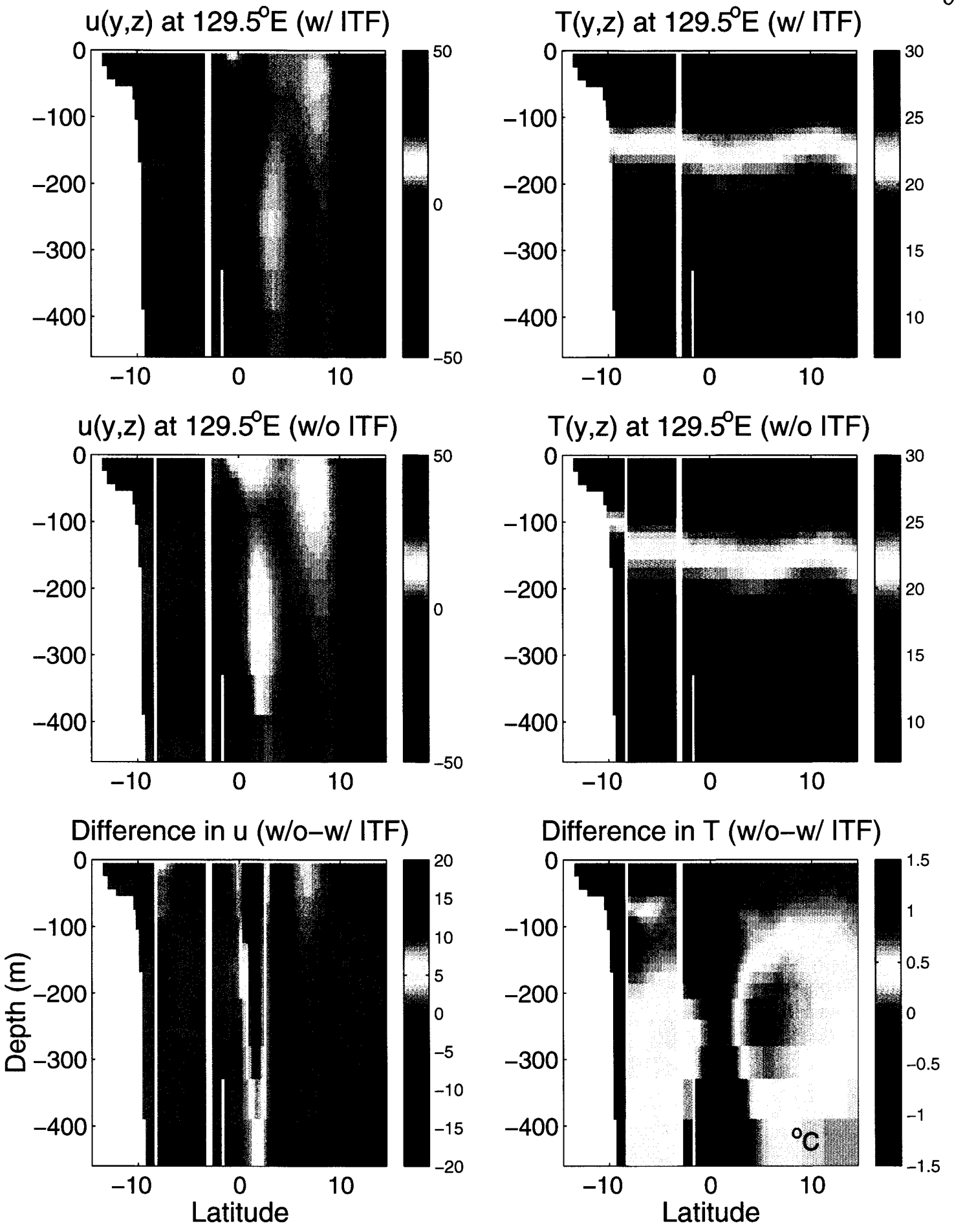
u(y,z) at 129.5°E (w/ ITF)
T(y,z) at 129.5°E (w/ ITF)
u(y,z) at 129.5°E (w/o ITF)
T(y,z) at 129.5°E (w/o ITF)
Difference in u (w/o–w/ ITF)
Difference in T (w/o–w/ ITF)
Depth (m)
Latitude
Latitude
°C
0
−100
−200
−300
−400
−10
0
10
50
0
−50
30
25
20
15
10
20
15
10
5
0
−5
−10
−15
−20
1.5
1
0.5
0
−0.5
−1
−1.5

Fig. 4

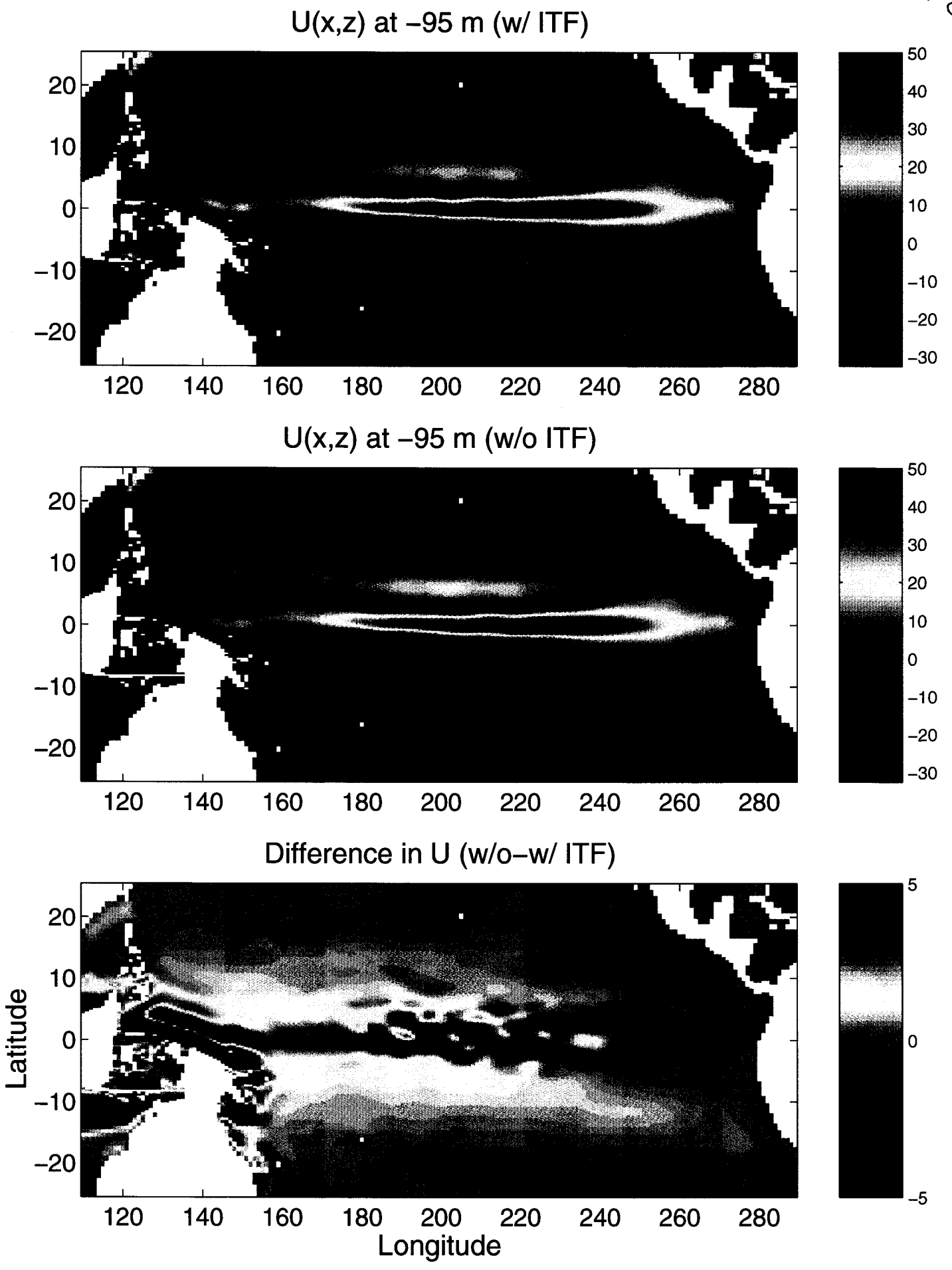
U(x,z) at −95 m (w/ ITF)
U(x,z) at −95 m (w/o ITF)
Difference in U (w/o−w/ ITF)
Latitude
Longitude
20
10
0
−10
−20
120
140
160
180
200
220
240
260
280
50
40
30
20
10
0
−10
−20
−30
5
0
−5

Fig. 5

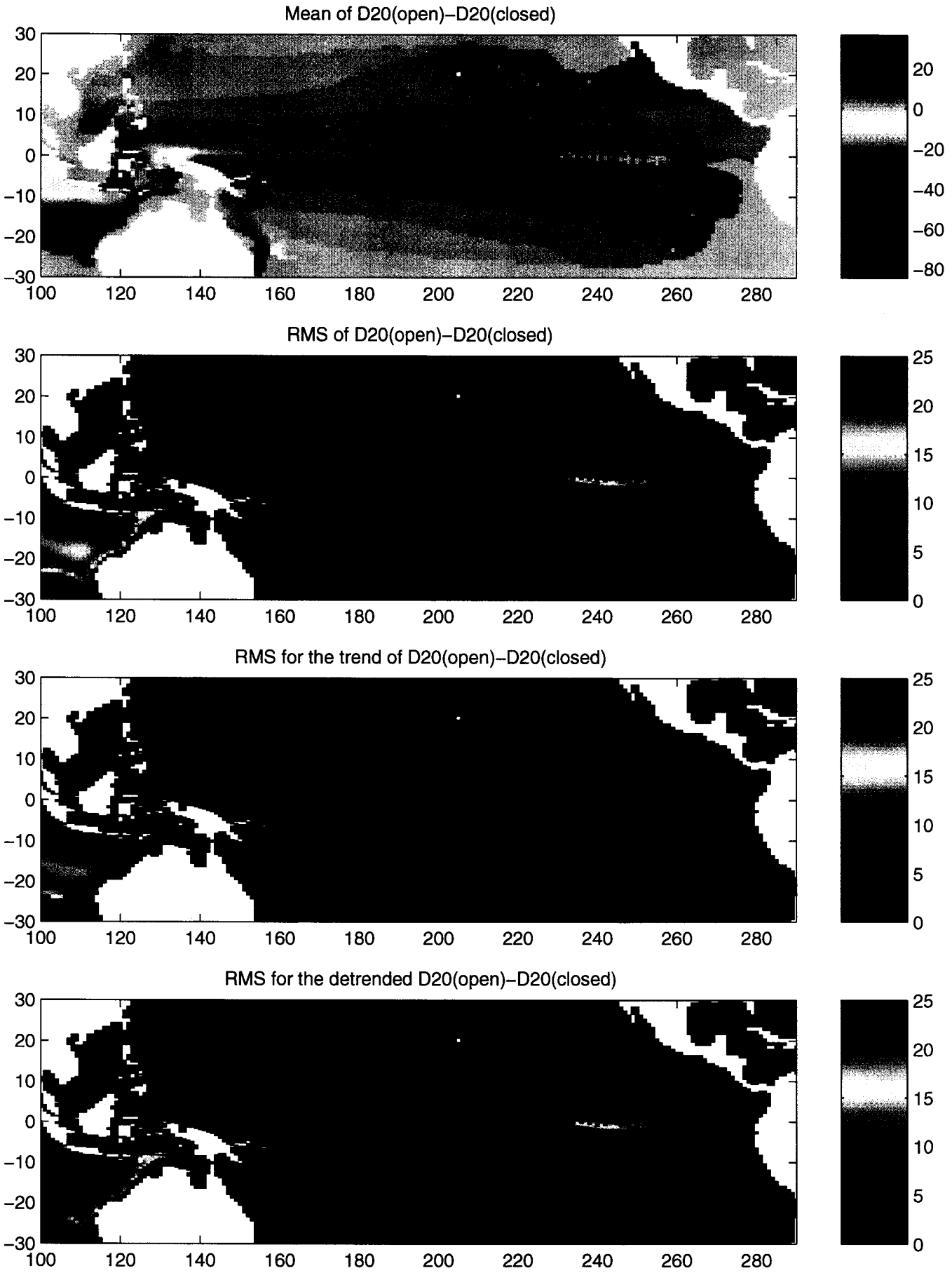
Mean of D20(open)–D20(closed)
RMS of D20(open)–D20(closed)
RMS for the trend of D20(open)–D20(closed)
RMS for the detrended D20(open)–D20(closed)
30
20
10
0
−10
−20
−30
100
120
140
160
180
200
220
240
260
280
20
0
−20
−40
−60
−80
25
20
15
10
5
0

Fig. 6

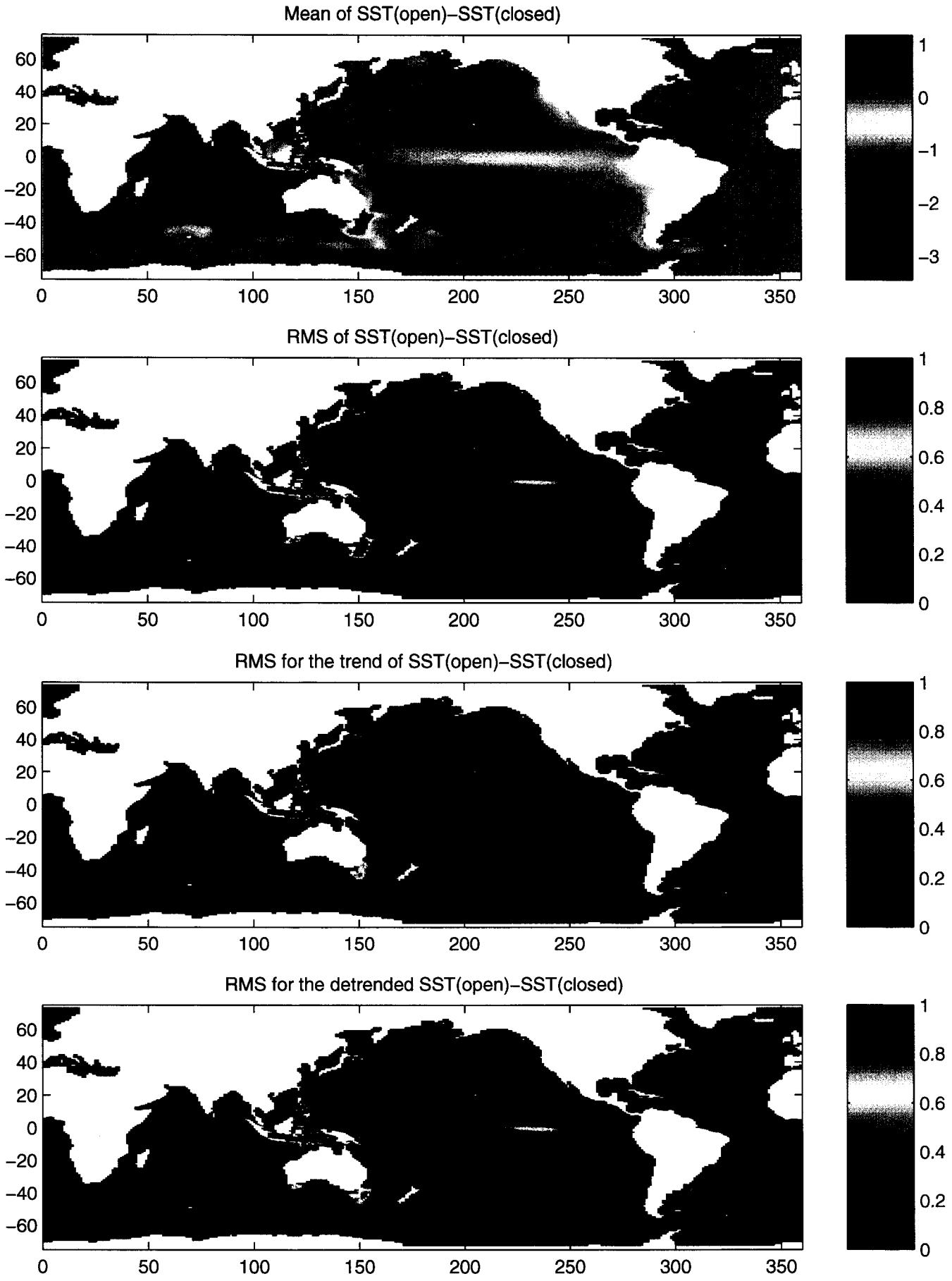
Mean of SST(open)–SST(closed)
RMS of SST(open)–SST(closed)
RMS for the trend of SST(open)–SST(closed)
RMS for the detrended SST(open)–SST(closed)
60
40
20
0
−20
−40
−60
0
50
100
150
200
250
300
350
1
0
−1
−2
−3
0.8
0.6
0.4
0.2